

POWDER METALLURGIC GIANT MAGNETOSTRICTION MATERIALS AND APPLICATION IN SPACE STRUCTURE

H. Eda¹, T. Mori², Y. Okada¹, L. Zhou¹ and J. Shimizu¹

¹*Department of Systems Engineering, Faculty of Engineering, Ibaraki University
12-1, Nakanaruswa, 4-chome, Hitachi-shi, 316-8511, Japan*

²*Material Research Center, TDK Corporation, Narita-shi, 286-8588, Japan*

TEL/FAX: +81-294-38-5188, E-mail: eda@hit.ipc.ibaraki.ac.jp

<http://pre-eng.admt.ibaraki.ac.jp>

Abstract

Powder metallurgic giant magnetostrictive materials (GMM) which are kind of metallic compounds creating magnetostrictive strain over several thousand ppm (parts per million). GMM is often used for positioning as well as vibration actuators with quick response and high repeatability. It is also believed that the high power and torque delivered by GMM in addition to the wide frequency range will open new possibilities for space applications. This paper describes a new process for manufacturing anisotropic GMM using powder metallurgic technique, and an application in vibration suppression for the space structures.

Keywords: giant magnetostrictive materials, powder metallurgy, rare-earth alloys, actuator, vibration suppression control system, space structure

Introduction

Conversion of electrical energy to mechanical energy in the presence of a magnetic field is the basic phenomenon of magnetostriction. Elongation or change in dimension occurs in GMM as a function of the external magnetic field applied. This elongation or force output is determined by the material crystal structure, which in turn depends on the elastic energy, magnetoelastic energy, directional and spin moment energy of the magnetrons, the phase and crystalline orientation, atomic vacancies, spin magnetic moment and the orbital magnetic moment.

Temperature variations disturbingly effect on the properties of the GMM. The problem is solvable through adjusting the composition ratio of elements used to produce GMM rod [1]. A new manufacturing process using powder metallurgic technique has been proposed in this article, and achieved great temperature stability. The GMM produced has a polycrystalline structure oriented to <111> axis, along which the effective magnetostriction takes place.

As one application of GMM, in this article, a vibration suppression device for space structures has been developed and examined. Simulation model of the control target and control logic have been proposed. From the results of both simulation and experimentation, quick vibration suppression has been realized.

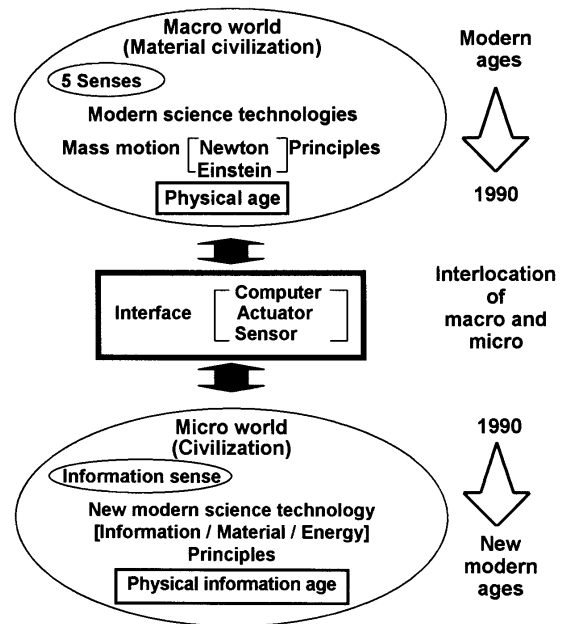


Figure 1 The world of the new generation

Background [2]

Figure 1 indicates the importance of the presence of an interface which connects a macro-world and a micro-world. The interface is mainly composed of actuators, sensors and microcomputers. As shown in Figure 2, it enables users to feel microscopic phenomenon as if they do in the macro-world.

In life science, medical, biological and space engineering, there are increasing demands of implementing fabrication, assembly, inspection, modification and/or evaluation at the micron or sub-micron scale^{[3], [4]}. To achieve this, development of new materials and devices, which are able to realize the required functions and movements at microscopic level, becomes mandatory. For instance, great power output, large displacement and quick response are often required for functional performances, while safety, stability and flexibility are the primary concern for structural applications. The gap between macro-world and micro-world needs to be bridged in a natural manner by utilizing advanced devices and smart materials. In these aspects, it is believed that giant magnetostrictive material

(GMM) is one of the most promising materials to satisfy such requirements.

Figure 3 illustrates evolution process of the intelligent system by means of unitizing microcomputers, actuators and sensors where the GMM plays a very important role.

Powder metallurgic GMM

As shown in the process flow of Figure 4, where (a) is Bridgman method and (b) is powder metallurgy method, the powder metallurgic process starts with the preparation of the alloy composite by milling the alloy ingots down to particles sized in 0.03-0.05 mm. Heat treatment is employed before and after the milling process, 14 hours at 950°C for crystal grain homogenization and 2.5 hours for the residual stress relief. Three different types of milled grain with the following composites are then blended together, and preformed in the presence of magnetic field of 96kA/m and at the pressure of 0.6MPa.

Alloy 1: $Tb_{0.4} Dy_{0.6} Fe_{1.95} + R_2O_3 + R_2C$

Alloy 2: $Dy_2 (Fe_{0.2}Co_{0.5}) + R_2O_3 + R_2C$

Raw material: $Fe + Fe_2O_3$

where, $R = Dy, Tb$

The developed structure is obtained in form of $Tb_{0.3} Dy_{0.7} (Fe_{1.85}Co_{0.06})$. The preformed materials is further sintered at the conditions of pressure = $6-12t/cm^2$ and temperature = $1180^\circ C$ for 1-3 hours in argon gas with the flow rate $2l/min$, followed by annealing at the temperature of $900^\circ C$ for 1 hour. As shown in Figure 5, the powder metallurgic GMM takes such a polycrystalline substance that the main phase RFe_2 grains are wrapped up with the R-rich layer and the oxide impurity as the grain boundary.

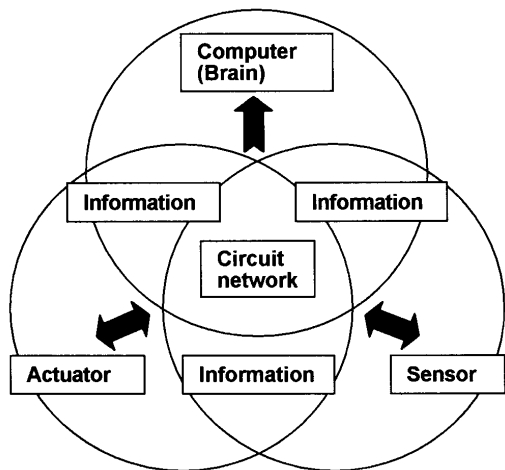


Figure 2 An intelligent system uniting actuator, sensor and computer

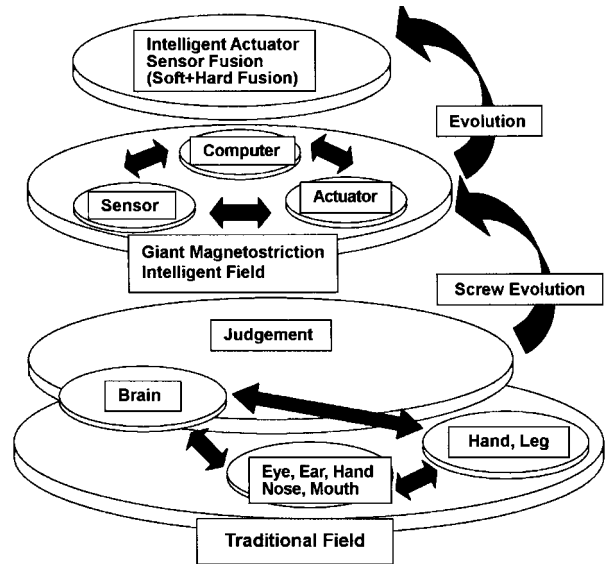
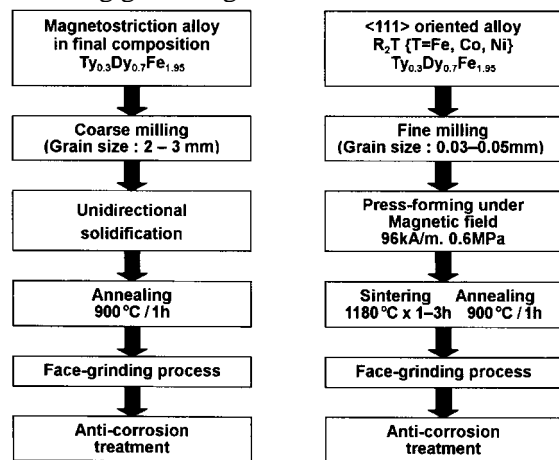


Figure 3 Evolution process in dynamical intelligent system using giant magnetostriction



(a) Bridgman method (b) powder metallurgy method
Figure 4 Fabrication processes of Bridgman method and powder metallurgy method

Since it is formed in the presence of a magnetic field, the powder metallurgic GMM has most of its crystals oriented to $\langle 111 \rangle$ direction. Figure 6 is the output chart of the X-ray diffraction in which the $\langle 111 \rangle$ oriented crystals is counted up to 38%. It means that the anisotropical composite has been managed in an appropriate crystal orientation along which the effective magnetostriction takes place.

Figure 7 compares the $S - H$ curves obtained by powder metallurgy and Bridgmen methods. Regardless of the pre-stress, the magnetostrictions obtained are quite comparable. So are the hystereses as well. It is particularly noteworthy that there is no initial "jump" observed in the powder metallurgic GMM. The other material properties are summarized in Table 1.

In addition to the manufacturing cost as low as 1/3 of conventional, the great advantage of the powder metallurgy is the capability of near-net-shape forming. Unlike the MB made GMM which is available only in right-angle cylinder form, the powder metallurgic GMM is able to be configured into any desired form as long as die-&-mold is applicable.

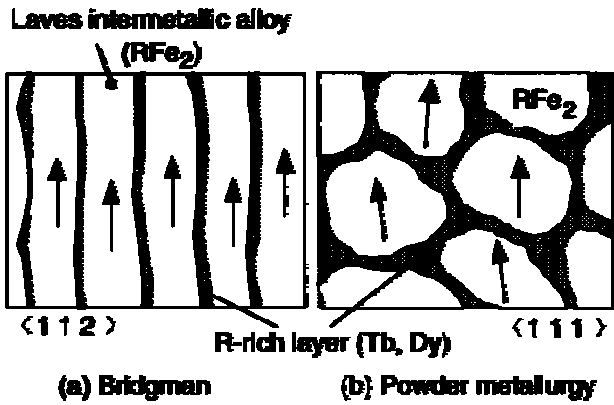


Figure 5 Crystal structure developed

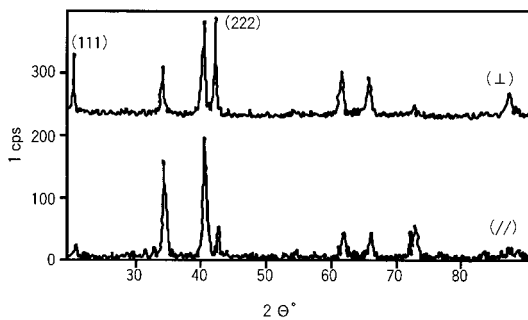


Figure 6 X-rays diffraction pattern of powder metallurgy GMM

Vibration suppression

The powder metallurgic giant magnetostrictive material (GMM) is characterized by high power, large displacement, fast response as well as safety, long lives and flexibility, which are often required by the aerospace structure. As one application of the giant magnetostrictive actuator, the vibration suppression for the aerospace structure has been explored. Described below are the design, simulation, the prototype development and simple suppression experiments.

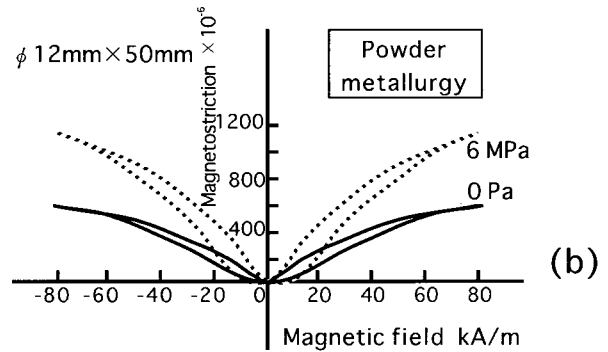
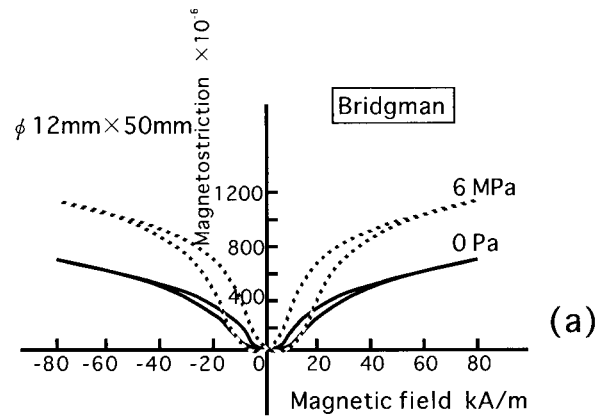


Figure 7 λ -H curves of $Tb_{0.3}Dy_{0.7}(Fe_{1.85}Co_{0.06})$ composite developed by Bridgman (a) and powder metallurgy (b) methods.

Table 1 Physical properties of produced GMM

| Property | Bridgman | PM |
|---|--------------------------|----------------------|
| Density ρ kg/m ³ | 9.20×10^3 | 7.56×10^3 |
| Elastic modulus E_r N/m ² *) | $3.8-4.0 \times 10^{10}$ | 3.7×10^{10} |
| Elastic modulus E_a N/m ² *) | $5.1-5.3 \times 10^{10}$ | 4.2×10^{10} |
| Bending strength kg/mm ² | 5.2 | 4.6 |
| Coupling coefficient k | 0.70 | 0.72 |
| Sonic velocity C_r m/s *) | 2088 | 2065 |
| Sonic velocity C_a m/s *) | 2426 | 2227 |
| Cost | 1 | 1/3 |

* r: parallel to anisotropic direction

a: vertical to anisotropic direction

Design of the suppression model

FEM is here used to study the dynamic characteristic of the suppression model and to design the control logic. It is however difficult to fully express the characteristics of the object at high frequency band. H_∞ robust control theory is then applied into the design of the controller.

For the simplicity, the object is approximated into a model with two degrees of freedom shown in Figure 8. The base part is free in gradient, while the tip mass is allowed to

move horizontally. The base and the tip mass are connected by a rigid beam, and the dynamic characteristics of the beam is not considered. The tip mass is idealized to a material particle and its gradient is ignored. In this model, the resonance mode appears only up to the secondary order. The modes of higher order are treated as the structural variation of the control object and the robust stabilization is applied with H^∞ control theory.

When θ_b is defined as the base gradient and x_m is as horizontal displacement of the tip mass, the motion equation of the base part at θ_b direction is given as;

$$J_b \ddot{\theta}_b = -M_0 + T - k_a \theta_b \quad (1)$$

where, J is the inertia moment of the base, T is the torque generated by the actuator, M_0 is the moment working on the root part of the beam and k_a is the rigidity of the actuator. The motion equation of the tip mass at x_m direction is express as;

$$m \ddot{x}_m = -F_1 \quad (2)$$

where, m is the mass, F_1 is the force component at x direction. When the displacements of the root and tip of the beam at x direction, and their gradients in respect to y axis are respectively defined as $x_0, \theta_0, x_1, \theta_1$, the force components at x direction and moments acting on the tip and root of the beam (F_0, M_0, F_1, M_1) can be expressed by the matrix of;

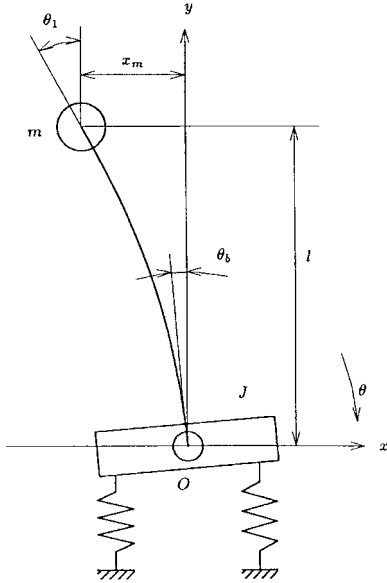


Figure 8 Schematic drawing of 2-DOF vibration model

$$\begin{bmatrix} F_0 \\ M_0 \\ F_1 \\ M_1 \end{bmatrix} = \begin{bmatrix} k_{11} & k_{12} & k_{13} & k_{14} \\ k_{21} & k_{22} & k_{23} & k_{24} \\ k_{31} & k_{32} & k_{33} & k_{34} \\ k_{41} & k_{42} & k_{43} & k_{44} \end{bmatrix} \begin{bmatrix} x_0 \\ \theta_0 \\ x_1 \\ \theta_1 \end{bmatrix} \quad (3)$$

where k_{ij} is the rigidity of each element and given as follows.

$$k = \begin{bmatrix} 12EI/l^3 & 6EI/l^2 & -12EI/l^3 & 6EI/l^2 \\ 6EI/l^2 & 4EI/l & -6EI/l^2 & 2EI/l \\ -12EI/l^3 & -6EI/l^2 & 12EI/l^3 & -6EI/l^2 \\ 6EI/l^2 & 2EI/l & -6EI/l^2 & 4EI/l \end{bmatrix} \quad (4)$$

where, E is the Young modulus of the beam, I is 2nd moment of area of the beam, and l is the length of the beam. Since $M_1 = 0$, $x_1 = x_m$ at the tip of the beam, and $x_0 = 0$, $\theta_0 = \theta_b$ at the root of the beam, θ_1 is given as;

$$\theta_1 = -\frac{k_{42}}{k_{44}} \theta_b - \frac{k_{43}}{k_{44}} x_m \quad (5)$$

Thus, it is able to calculate the moment M_0 working at the base and the force component F_1 working at the tip as follows;

$$\begin{aligned} M_0 &= k_{22} \theta_b + k_{23} x_m + k_{24} \theta_b \\ &= \left(k_{22} - k_{24} \frac{k_{42}}{k_{44}} \right) \theta_b + \left(k_{23} - k_{24} \frac{k_{43}}{k_{44}} \right) x_m \end{aligned} \quad (6)$$

$$\begin{aligned} F_1 &= k_{32} \theta_b + k_{33} x_1 + k_{34} \theta_1 \\ &= \left(k_{32} - k_{34} \frac{k_{42}}{k_{44}} \right) \theta_b + \left(k_{33} - k_{34} \frac{k_{43}}{k_{44}} \right) x_m \end{aligned} \quad (7)$$

Therefore, the motion equations result in;

$$J_b \ddot{\theta}_b = -\left(k_{22} - k_{24} \frac{k_{42}}{k_{44}} + k_a \right) \theta_b - \left(k_{23} - k_{24} \frac{k_{43}}{k_{44}} \right) x_m + T \quad (8)$$

$$m \ddot{x}_m = -\left(k_{32} - k_{34} \frac{k_{42}}{k_{44}} \right) \theta_b - \left(k_{33} - k_{34} \frac{k_{43}}{k_{44}} \right) x_m \quad (9)$$

when the quantity of state is made as

$$x = \begin{bmatrix} \theta_b & \dot{\theta}_b & x_m & \dot{x}_m \end{bmatrix}^T, \text{ the state equation is given}$$

as:

$$\begin{aligned} \dot{x} &= A_p x + B_p u \\ y &= C_p x + D_p u \end{aligned} \quad (10)$$

$$A_p = \begin{bmatrix} 0 & 1 & 0 & 0 \\ -(k_{22} - k_{42}k_{24}/k_{44} + k_a)/J & 0 & -(k_{23} - k_{43}k_{24}/k_{44})/J & 0 \\ 0 & 0 & 0 & 1 \\ -(k_{32} - k_{43}k_{24}/k_{44})/m & 0 & -(k_{33} - k_{34}k_{43}/k_{44})/m & 0 \end{bmatrix}$$

$$B_p = \begin{bmatrix} 0 \\ 1/J \\ 0 \\ 0 \end{bmatrix}, \quad C_p = \begin{bmatrix} 1 & 0 & 0 & 0 \\ 0 & 0 & 1 & 0 \end{bmatrix}, \quad D_p = 0$$

Each parameter used is listed in table 2.

Table 2 Parameters

| | | | |
|------------|--------------------------------------|------------|-------------------------------------|
| J | $4000 \times 10^{-4} [\text{kgm}^2]$ | E | $7.5 \times 10^{10} [\text{N/m}^2]$ |
| I | $4.2 \times 10^{-9} [\text{m}^4]$ | l | $1.5 [\text{m}]$ |
| m | $2.2 [\text{kg}]$ | k_a | $7 \times 10^3 [\text{Nm/rad}]$ |
| ω_1 | $10.8 [\text{rad/sec}]$ | ω_2 | $138 [\text{rad/sec}]$ |

Controller design

The following facts are especially taken into the consideration for the design of the controller.

- the resonant vibration of 1st and 2nd mode
- the instability at higher resonance mode

Taking W_S (weight for control performance), W_T as the multiplicative fluctuation weights at the input side, the plant is generalized as shown in Figure 9. Here the w_1 is the external force and w_2 is the sensor noise. The state equation of the plant is as;

$$\begin{aligned} \dot{x} &= A_p x + B_p (w_1 + u) \\ y &= C_p x + D_w w_2 \end{aligned} \quad (11)$$

Here, D_w is the weight of the disturbance, which is added to meet the condition for solving the H^∞ standard problem,

$$D_w = \begin{bmatrix} 1 \times 10^{-4} & 0 \\ 0 & 1 \times 10^{-5} \end{bmatrix} \quad (12)$$

When the weights W_S , W_T respectively take value of;

$$W_S = \begin{bmatrix} A_S & B_S \\ C_S & D_S \end{bmatrix} \quad W_T = \begin{bmatrix} A_T & B_T \\ C_T & D_T \end{bmatrix}$$

the generalized plant is given as;

$$G(s) = \begin{bmatrix} A & B_1 & B_2 \\ C_1 & D_{11} & D_{12} \\ C_2 & D_{21} & D_{22} \end{bmatrix} = \begin{bmatrix} A_S & 0 & B_S C_p & 0 & B_S D_w & 0 \\ 0 & A_T & 0 & 0 & 0 & B_T \\ 0 & 0 & A_p & B_p & 0 & B_p \\ C_S & 0 & D_S C_p & 0 & D_S D_w & 0 \\ 0 & C_T & 0 & 0 & 0 & D_T \\ 0 & 0 & C_p & 0 & D_w & 0 \end{bmatrix} \quad (13)$$

The solution of this generalized plant is found by using the robust control toolbox of MATLAB. As a result of trial-and-error, the following W_S and W_T were chosen to control the resonant vibration. Then the solution was obtained at $\gamma = 62$ and the controller is also obtained. The transfer characteristic of the controller is shown in Figure 10.

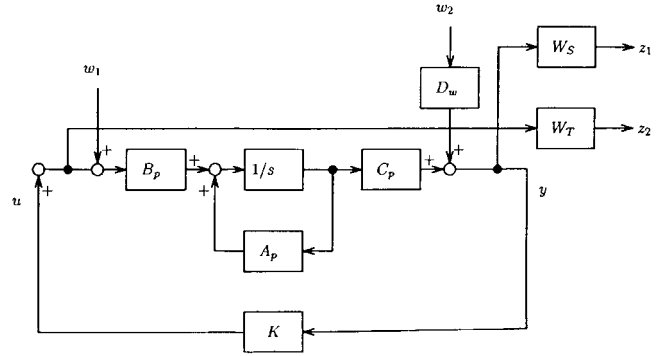


Figure 9 Generalized plant

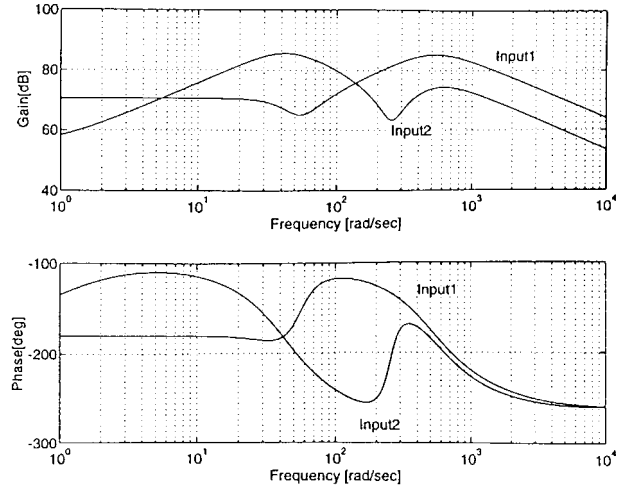


Figure 10 Bode diagram of controller

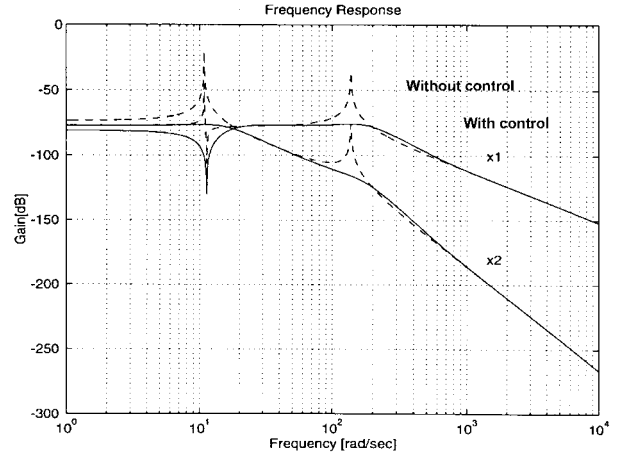


Figure 11 Gain diagram of frequency response

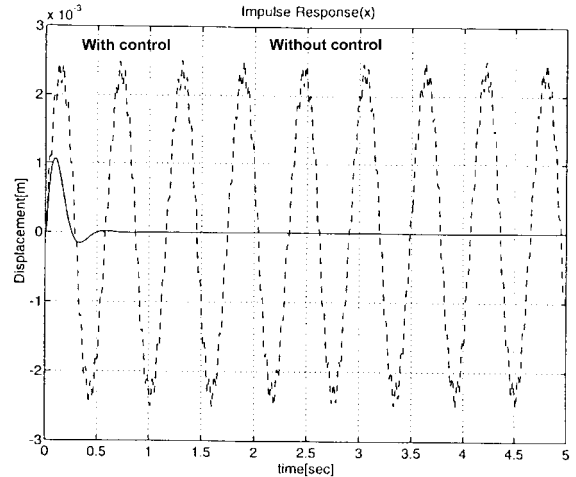


Figure 12 Impulse response

By applying the sine wave excitation to the base, the frequency response of the controller designed above was studied. The gain chart is shown in Figure 11, with the dot line for non-control and solid line for controlled results. It is obvious from the chart that the first and secondary resonance is effectively controlled. The time response of the tip mass, as an impulse input is given to the base, is shown in Figure 12, with the dot line for non-control and solid line for controlled results. It shows that the control converges the vibration in a short time. The above simulation results confirmed that the controller with the H^∞ control was effective for the vibration suppression.

Outline of the prototype

The prototype of the vibration suppression device is schematically in Figure 13. The beam is made of aluminum material, with the first resonant frequency about 3Hz or lower and the acceleration at the tip 1G or less. The beam is vertically held by a single-end supporter shown in Figure 14. The mass is added to the beam tip accordingly. Prior to starting the suppression, excitation can be applied to the device if necessary. The suppression device consists of a giant magnetostrictive actuator mechanism, electronic equipment for the control, measuring instrument. A pin hinge is built in the beam supporter. By the paired giant magnetostrictive actuator, the controllable force around the pin hinge is generated. Parameters measured are acceleration of the beam tip, strain of the beam root, displacement of the magnetostrictive actuator, any of them can be used as input signal to be fed back the control system.

Result and discussion

The vibration suppression experiment was carried out at the prototype device without doing the feedback control, but inputting a proper sine wave corresponding to the resonance frequency and in opposite phase of the vibration detected from the signal of the accelerometer. The control was continued until the vibration (the maximum acceleration) was constantly below a specified level.

The beam was first excited from a standstill state by applying into the magnetostrictive actuators a sine wave current (maximum 3A) with the first order frequency of the beam. The suppression was then started from the steady state of vibration, by giving the actuators a maximum 4A current whose phase was inverted from that of the input current.

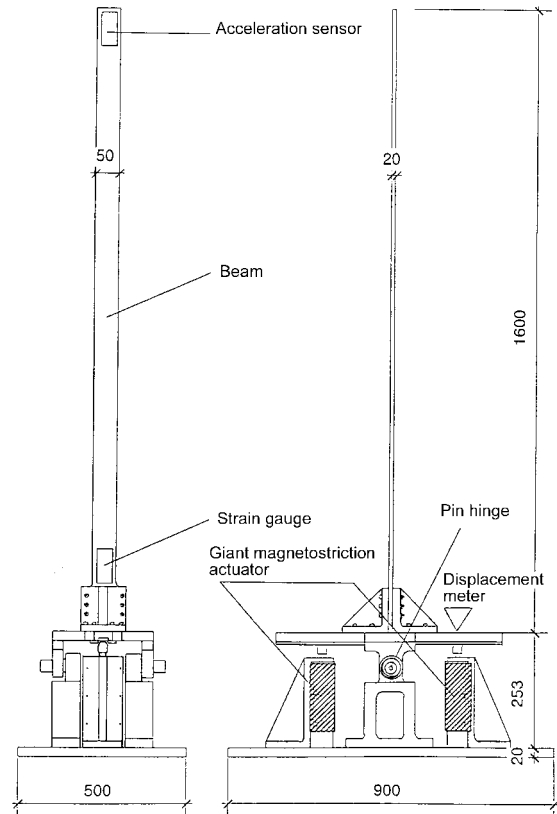


Figure 13 Schematic drawing of the prototype

In order to compensate the phase deviation taking place during the suppression, the phase of suppression current was corrected every few seconds according to the information from the accelerometer. Figure 15 is the time history of the acceleration at the tip of beam and the suppression current input into the actuators. The beam tip acceleration has dramatically decreased in about 10 seconds after the suppression started

Conclusion

This paper described the properties of the giant magnetostrictive materials made by powder metallurgy and its potential applications for the aerospace structure. The results achieved can be summarized as follows; In addition to the magnetostrictive property as good as that made by the Bridgman Method (Terfenor-D), the powder metallurgy process is able to produce good isotropic components by not applying the magnetic field during the compression. Also nearly perfect anisotropic components can be quickly and inexpensively produced into various sizes and shapes without scarifying performances. The powder metallurgic magnetostrictive materials are sort of promising material for various future devices.

- (1) At the development of the vibration suppression device for aerospace structure, it has been confirmed from the simulation and experiment that proposed GMM actuator is able to perform an effective and fast suppression.
- (2) The prototype developed has verified the potential and effectiveness of powder metallurgic GMM actuator in the application to the aerospace industry.

Acknowledgement

This prototype was developed as a part of the project organized by the Society for Non-Traditional Technology and founded by NASDA (National Space Development Agency of Japan), and Grand-in-Aid for Exploratory Research (No.10875029).

References

- [1] A. E. Clark, Magnetostrictive Rare Earth Fe Compounds Naval Surface Warfare Center, Edited by E. P. Wohlfarth, (USA), (1980), 533
- [2] H. Eda, "New techno-world of machine tool and production processing evolution (Giant magnetostrictive material for innovation of intellectualized actuators and sensors)", Transaction of the Japan Society of Mechanical Engineers, 63 - 610 C (1997) pp.3321-3326.

[3] Marc Madou: Fundamentals of Micro Fabrication, CRC press, 1997

[4] L. Chouanine, H. Eda and J. Shimizu: Development of Key-Technology on the State-of-the art Machine Tool and Generalization of Grinding Forces under Ductile Mode Grinding Experiments, Int. Journal of JSPE, 32 2(1998), 98-103.

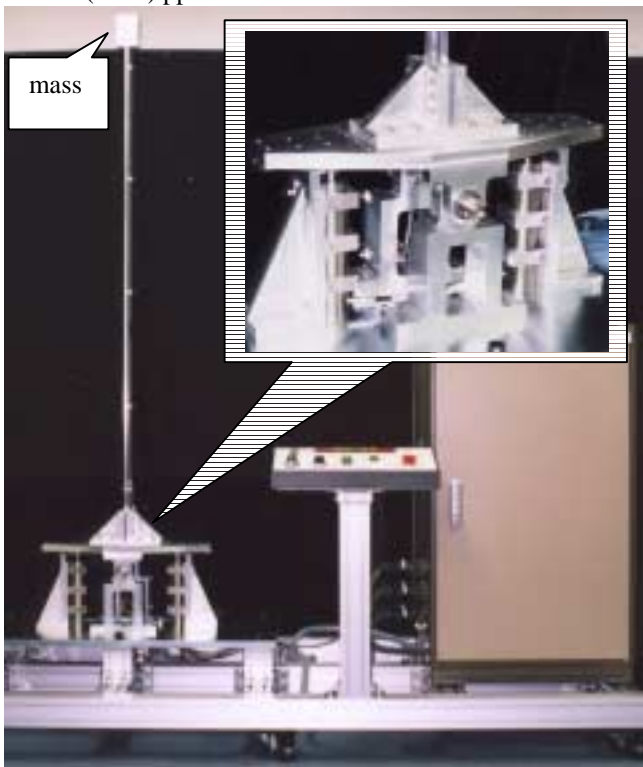


Figure 14 Prototype developed

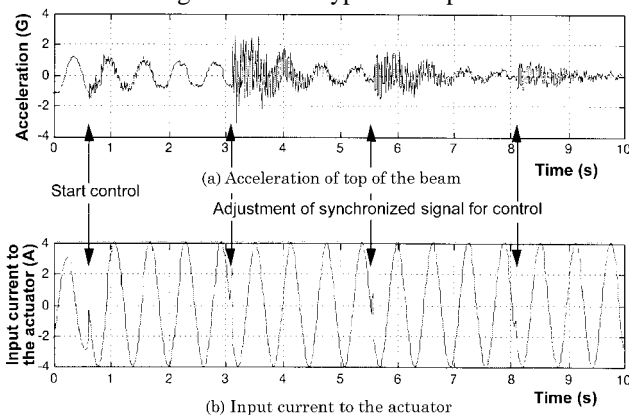


Figure 15 An example of experimental result in vibration suppression

